Low frequency of intracranial progression in advanced NSCLC patients treated with cancer immunotherapies

Short Title: Cancer immunotherapy and intracranial progression

Authors: Naoya Kemmotsu[1,2], Kiichiro Ninomiya[3], Kei Kunimasa[4], Takamasa Ishino[1], Joji Nagasaki[1], Yoshihiro Otani[2], Hiroyuki Michiue[2,5], Eiki Ichihara[3], Kadoaki Ohashi[3], Takako Inoue[4], Motohiro Tamiya[4], Kazuko Sakai[6], Youki Ueda[1], Hiromichi Dansako[1], Kazuto Nishio[6], Katsuyuki Kiura[3], Isao Date[2], and Yosuke Togashi[1#]

Affiliations: [1]Department of Tumor Microenvironment, [2]Department of Neurological Surgery, and [3]Department of Respiratory Medicine, Faculty of Medicine, Dentistry and Pharmaceutical Sciences, Okayama University, Okayama, Japan; [4]Department of Thoracic Oncology, Osaka International Cancer Institute, Osaka, Japan; [5]Neutron Therapy Research Center, Okayama University, Okayama, Japan; [6]Department of Genome Biology, Kindai University Faculty of Medicine, Osaka-Sayama, Japan.

#Corresponding Author:
Yosuke Togashi (0000-0001-9910-0164), Department of Tumor Microenvironment, Okayama University Graduate School of Medicine Dentistry and Pharmaceutical Sciences, 2-5-1 Shikata-cho, Kita-ku, Okayama 700-8558, Japan.
Phone: +81-86-235-7390; Fax: +81-86-235-7392; E-mail: ytogashi@okayama-u.ac.jp

Key words: non-small-cell lung cancer; cancer immunotherapy; intracranial metastasis; intracranial progression; memory precursor effector T cell.

List of Abbreviations:
BBB, blood–brain barrier; CNS, central nervous system; EGFR-TKIs, epidermal growth factor receptor-tyrosine kinase inhibitor; ICI, immune checkpoint inhibitors; mAbs, monoclonal antibodies; MPEC, memory precursor effector cells; NSCLC, non-small-cell lung cancer; OVA, ovalbumin; OS, overall survival; PFS, progression-free survival; SQ, squamous; TILs, tumor-infiltrating lymphocyte

The appropriate article category; Research Articles

What's New:
The frequency of intracranial progression in advanced non-small-cell lung cancer patients treated with PD-1 blockade therapies was significantly lower than that in patients treated with cytotoxic chemotherapies. In murine models, PD-1 blockade suppressed intracranial rechallenged tumors after initial rejection and induced long-lived memory T cells and antigen-specific T cells in intracranial lesions. These findings suggest that cancer immunotherapies can prevent intracranial progression and maintain long-term effects both intracranially and systemically.

Abstract

Intracranial metastases are common in non-small-cell lung cancer (NSCLC) patients, whose prognosis is very poor. In addition, intracranial progression is common during systemic treatments due to the inability to penetrate central nervous system (CNS) barriers, whereas the intracranial effects of cancer immunotherapies remain unclear. We analyzed clinical data to evaluate the frequency of intracranial progression in advanced NSCLC patients treated with PD-1 blockade therapies compared with those treated without PD-1 blockade therapies, and found that the frequency of intracranial progression in advanced NSCLC patients treated with PD-1 blockade therapies was significantly lower than that in patients treated with cytotoxic chemotherapies. In murine models, intracranial rechallenged tumors after initial rejection by PD-1 blockade were suppressed. Accordingly, long-lived memory precursor effector T cells and antigen-specific T cells were increased by PD-1 blockade in intracranial lesions. However, intracranial rechallenged different tumors are not suppressed. Our results indicate that cancer immunotherapies can prevent intracranial progression, maintaining long-term effects intracranially as well as systemically. If intracranial recurrence occurs during the treatment with PD-1 blockade therapies, aggressive local therapies could be worthwhile.

Introduction

Intracranial metastases are common in cancer patients, occurring in 10% to 30% of patients [1-5]. The incidence of intracranial metastases is increasing because of advances in the treatment of primary tumors, decreased mortality, and technical advances in neuroimaging. The most common source of intracranial metastases is non-small-cell lung cancer (NSCLC), and the median survival of NSCLC patients with untreated intracranial lesions is a mere 1–2 months [6]. Cytotoxic chemotherapy and molecular-targeted therapies, such as platinum doublets and epidermal growth factor receptor tyrosine kinase inhibitors (EGFR-TKIs), have been commonly used for NSCLC, but the efficacies of these therapies against intracranial lesions are reportedly limited due to the inability to penetrate central nervous system (CNS) barriers [1-5, 7]. Furthermore, many studies have demonstrated that intracranial progression is common during these treatments due to these barriers [8, 9].

Immune checkpoint inhibitors (ICIs), such as monoclonal antibodies (mAbs)

against PD-1/PD-L1, have been approved for the treatment of various cancer types, including NSCLC, leading to a paradigm shift in cancer therapy [10]. ICIs exhibit efficacy via the reactivation of effector T cells [11]. In addition, durable responses to ICIs are observed in some patients, and differentiation into long-lived memory T cells can play important roles in such durable responses [12-15]. Regarding intracranial lesions, it has been reported that ICIs are effective for intracranial metastases [16-20], and another study has shown that the frequency of intracranial progression seems not to be high compared with other organs during treatment with PD-1 blockade therapies [21]. These findings indicate that ICI therapy can differ from other systemic therapies, such as cytotoxic chemotherapies and/or molecular-targeted therapies, in efficacy against intracranial lesions.

Here, we analyzed the clinical data of NSCLC patients and found that the frequency of intracranial progression in NSCLC patients treated with PD-1 blockade therapies was significantly lower than that in patients treated with cytotoxic chemotherapies. Furthermore, we conducted several mouse experiments including tumor-

rechallenging murine models for intracranial lesions and analyzed long-lived memory T cells and antigen-specific T cells to investigate the mechanisms.

Materials and methods

Patients.

Seventy-four advanced NSCLC patients who participated in an observational study of PD-1 blockade therapies without anti-CTLA-4 mAb as first-line therapy from 2017 to 2020 were enrolled as the ICI cohort. In addition, 80 advanced NSCLC patients who participated in two trials evaluating the tolerability of cisplatin-based chemotherapies as first-line therapy from 2010 to 2014 were enrolled in this study as the non-ICI cohort [22, 23]. Before the initiation of first-line therapies, *EGFR* status was analyzed in all patients; however, *ALK* status was not analyzed in 22 patients. All patients underwent magnetic resonance imaging (MRI) to identify initial intracranial lesions, abdominal computed tomography (CT) for initial liver metastases, and bone scintigraphy or positron emission tomography CT (PET-CT) for initial bone metastases. *EGFR*-mutated, *ALK*-fused, or

ALK-unknown NSCLC patients and patients who initially had some symptoms due to intracranial lesions were excluded from these two cohorts (**Supplementary Table S1**).

Follow up

MRI of the brain was performed before and at least every six months after chemotherapy. Similarly, abdominal CT was performed before and at least every three months after chemotherapy. However, bone metastases were not evaluated periodically during the follow-up. To evaluate disease progression, the Response Evaluation Criteria in Solid Tumors (RECIST; ver. 1.1) was applied. For clinical intracranial progression, an event was defined as the date of imaging.

Cell lines and reagents.

The LL/2 (murine lung cancer; RRID: CVCL_4358) cell line was purchased from ATCC (Manassas, VA). The MC-38 cell line (murine colon cancer; RRID: CVCL_B288) was obtained from Kerafast (Boston, MA). These cell lines were maintained in RPMI 1640 and DMEM (FUJIFILM Wako Pure Chemical Corporation, Osaka, Japan) supplemented

with 10% foetal bovine serum (FBS; Thermo Fisher Science, Waltham, MA). All experiments were performed with mycoplasma-free cells. Rat anti-mouse PD-1 mAb (RMP1-14) and control rat IgG2a mAb (RTK2758) were obtained from BioLegend (San Diego, CA).

Constructs, virus production, and transfection.

Ovalbumin (OVA) cDNA was subcloned into pBABE-puro (Addgene, Watertown, MA). pBABE-puro was a gift from Hartmut Land & Jay Morgenstern & Bob Weinberg (Addgene plasmid # 1764; http://n2t.net/addgene:1764; RRID: Addgene_1764) [24]. pHAGE PGK-GFP-IRES-LUC-W (Luc) vector was purchased from Addgene (RRID: Addgene_46793). pHAGE PGK-GFP-IRES-LUC-W was a gift from Darrell Kotton (Addgene plasmid # 46793; http://n2t.net/addgene:46793; RRID: Addgene_46793) [25]. These virus vectors were transfected into packaging cells using Lipofectamine 3000 Reagent (Thermo Fisher Scientific). After 48 hours, the supernatant was concentrated and transfected into cells.

***In vivo* animal models.**

Female C57BL/6J mice (6-8 weeks old) were purchased from SLC Japan (Shizuoka, Japan). Tumor cells (5×10^5) were inoculated subcutaneously, and tumor volume was monitored every three days. The means of the long and short diameters were used to generate tumor growth curves. To generate intracranial tumors, tumor cells (2×10^5) were stereotactically injected into the striatum (2 mm right from the midline, 2 mm anterior to bregma, 3 mm deep). For the imaging of intracranial tumors, Luc-overexpressing cells were used, and anesthetized mice were injected with luciferin substrate (Xenogen, Alameda, CA). A series of bioluminescent images were then taken for up to 30 minutes using a Xenogen IVIS Lumina system. Photon output was quantified at the plateau of the time course using Living Image 3.0 (Xenogen). Anti-PD-1 mAb (200 μg/mouse) or control mAb was administered intraperitoneally three times every three days thereafter. Furthermore, we performed tumor-rechallenging mouse experiments. Briefly, mice that had completely eradicated the initial subcutaneous tumors after anti-PD-1 mAb were secondarily challenged with tumor cells subcutaneously or intracranially on Day 32. Tumors were harvested 14 days after tumor cell inoculation to collect tumor-infiltrating

lymphocytes (TILs) for evaluation by flow cytometry. All *in vivo* experiments were performed at least twice. All mice were maintained under specific pathogen-free conditions in the animal facility of the Institute of Biophysics.

Flow cytometry analyses.

Flow cytometry assays were performed as previously described [26, 27]. Briefly, cells were washed with PBS containing 2% FBS and subjected to staining with surface antibodies and an H2-Kb/OVA-specific dextramer. The samples were assessed with a FACS Fortessa (BD Biosciences) and FlowJo software (BD Biosciences). The staining antibodies were diluted following the manufacturer's instructions. The antibodies and dextramer used in the flow cytometry analyses are summarized in **Supplementary Table S2**.

Statistical analysis.

GraphPad Prism 8 (GraphPad Software, San Diego, CA) was used for statistical analyses. The relationships between groups were compared using Fisher’s exact test. The relationships of continuous variables between groups were compared using the t test. The

191 relationships between tumor volume curves were compared using two-way analysis of
192 variance (ANOVA). Overall survival (OS), intracranial, hepatic, and bone progression-
193 free survival (PFS) were defined as the time from the initiation of first-line standard
194 chemotherapy to death from any cause, the time from the initiation of first-line standard
195 chemotherapy to the first observation of intracranial disease progression or death from
196 any cause, the time from the initiation of first-line standard chemotherapy to the first
197 observation of hepatic disease progression or death from any cause, and the time from the
198 initiation of first-line standard chemotherapy to the first observation of bone disease
199 progression or death from any cause, respectively. In addition, because this study
200 compared two cohorts with different enrollment times, the observation period was
201 censored at 36 months to avoid the lead-time bias between the groups. OS and intracranial
202 PFS were analyzed using the Kaplan–Meier method and compared among groups using
203 the log-rank test. All tests were 2-tailed, and *P value*s < 0.05 were considered statistically
204 significant.
205
206

Results

Patients with NSCLC who receive PD-1 blockade therapies have a lower frequency of intracranial progression.

First, we analyzed our original two cohorts to elucidate the impact of immunotherapies on the frequency of intracranial progression. We retrospectively collected the clinical data of advanced NSCLC patients who received immunotherapies as first-line therapy from 2017 to 2020 (ICI cohort). During the same period, only 10 patients with advanced NSCLC without *EGFR* mutations or *ALK* fusions received platinum doublet chemotherapy without ICIs as first-line therapy. In addition, nine of the ten patients had autoimmune diseases. It may be difficult to compare the clinical data between the ICI cohort and the small non-ICI cohort with autoimmune diseases. Thus, to collect clinical data of patients who had never received any immunotherapies, we used a cohort (non-ICI) including advanced NSCLC patients who received standard cisplatin-based chemotherapies as first-line therapy from 2010 to 2014. In this cohort, none of the patients received immunotherapies because ICIs were not approved in Japan during this period. From these two cohorts, *EGFR*-mutated, *ALK*-fused, or *ALK*-unknown NSCLC

patients were excluded because such driver gene alterations could have a biological effect on intracranial lesions, and ICIs generally exhibit less efficacy in such patients [28-30]. In addition, patients who initially had some symptoms due to intracranial lesions were also excluded, resulting in 32 and 54 patients in the non-ICI cohort and the ICI cohort, respectively.

The clinical characteristics are summarized in **Supplementary Table S1**. While the non-ICI cohort included younger patients and more nonsquamous (non-SQ) histology than the ICI cohort, there was no significant difference in initial intracranial lesions between the two cohorts (**Supplementary Table S1**). Eighteen patients received PD-1 blockade monotherapy because they had high PD-L1 expression ($\geq$ 50%), and the others received combined PD-1 blockade therapies with platinum doublet (**Supplementary Table S1**). As shown in **Figure 1A**, the frequency of intracranial progression was significantly higher in the non-ICI cohort than in the ICI cohort. In addition, significant intracranial tumor regression and long-term intracranial PFS were observed in several patients with initial intracranial lesions in the ICI cohort (**Supplementary Fig. S1**). Since squamous (SQ) histology was dominant in the ICI cohort and the difference in histology

239 could have an influence on intracranial recurrence, we next focused on patents with
240 nonsquamous cell carcinoma (non-SQ). Similarly, the frequency of intracranial
241 recurrence was significantly higher in the non-ICI cohort than in the ICI cohort (**Fig. 1B**).
242 In addition, focusing on patients with no initial intracranial lesions, the frequency of
243 intracranial progression was significantly higher in the non-ICI cohort (**Fig. 1C**). In
244 addition, the frequency of intracranial progression was significantly higher in non-SQ
245 patients without initial intracranial lesions in the non-ICI cohort (**Supplementary Fig.**
246 **S2A**). However, when the 18 patients who received ICI monotherapy were excluded from
247 the ICI cohort, there was a trend toward a higher frequency of intracranial progression in
248 the non-ICI cohort; however, the difference was not significant (**Supplementary Fig.**
249 **S2B**). These findings suggest that ICIs could prevent intracranial progression in NSCLC
250 compared with cytotoxic chemotherapies.

251 Liver and bone metastases were also analyzed in the same cohort. There were no
252 significant differences in the initial hepatic or bone lesions between the two cohorts
253 (**Supplementary Table S1**). There was a trend toward a higher frequency of hepatic
254 progression in the non-ICI cohort; however, the difference was not significant

(**Supplementary Fig. S2C**). Due to the difficulty of evaluating bone metastases with RECIST as target lesions, patients with initial bone lesions were excluded for bone progression. There was a trend toward a higher frequency of bone progression in the non-ICI cohort; however, the difference was not significant (**Supplementary Fig. S2D**). Overall survival in the ICI cohort tended to be longer, but not significantly longer, than that in the non-ICI cohort (**Supplementary Fig. S2E**). These results suggest that ICIs may inhibit hepatic and bone progression, but not as markedly as its effect on intracranial progression.

PD-1 blockade exhibits efficacy against intracranial tumors in mouse models.

To gain further insights into intracranial lesions, we performed several mouse experiments using OVA-overexpressing LL/2 (LL/2-OVA) and MC-38 cell lines. These subcutaneous tumors were sensitive to PD-1 blockade (**Fig. 2A** and **Supplementary Fig. S3A**). A reporter vector (Luc vector) was introduced into both cell lines, and luciferase activity was analyzed with IVIS to evaluate the intracranial efficacies. Then, we inoculated these tumor cells into the mouse brain and treated them with an anti-PD-1

mAb. As shown in **Figure 2B** and **Supplementary Fig. S3B**, intracranial tumors were sensitive to PD-1 blockade. Accordingly, PD-1 blockade increased the proportions of $CD62L^{-}CD44^{+}CD8^{+}$ effector T cells and $PD\text{-}1^{+}CD8^{+}$ T cells in intracranial LL/2-OVA/Luc tumors, as was observed in subcutaneous tumors (**Fig. 2C, D** and **Supplementary Fig. S4**). These findings suggest that PD-1 blockade exhibits efficacy against intracranial and systemic lesions by activating effector T cells.

Initial rejection of subcutaneous mouse tumors after treatment with PD-1 blockade suppresses subcutaneous rechallenge of the same tumors.

Next, we performed tumor-rechallenging experiments. Briefly, mice that had completely eradicated the initial subcutaneous tumors after anti–PD-1 mAb were rechallenged with the same tumor cells, subcutaneously (**Fig. 3A**). After complete eradication treated with PD-1 blockade, most of the subcutaneous rechallenged tumors were completely rejected (**Fig. 3B** and **Supplementary Fig. S5A**). Since memory precursor effector cells (MPECs) generate long-lived $CD8^{+}$ memory T cells [31], we analyzed the proportion of MPECs in tumors. These cells reportedly express high levels

of CD127 and low levels of KLRG1. After PD-1 blockade, the proportion of MPECs increased in subcutaneous LL/2-OVA tumors (**Fig. 3C**). In addition, the proportion of H2-Kb/OVA-specific dextramer^{+}CD8^{+} T cells also increased (**Fig. 3D**).

Initial rejection of subcutaneous mouse tumors after treatment with PD-1 blockade suppresses intracranial rechallenge of the same tumors.

Furthermore, we performed intracranial tumor-rechallenging experiments. Briefly, mice that had completely eradicated the initial subcutaneous tumors after anti–PD-1 mAb were rechallenged with the same tumor cells intracranially (**Fig. 4A**). After complete eradication and treatment with PD-1 blockade, intracranial rechallenged tumors were suppressed (**Fig. 4B** and **Supplementary Fig. S5B**), which is similar to subcutaneous rechallenged tumors. Accordingly, PD-1 blockade increased the proportions of MPECs and H2-Kb/OVA-specific dextramer^{+}CD8^{+} T cells in intracranial LL/2-OVA/Luc tumors, as was observed in subcutaneous tumors (**Fig. 4C** and **D**). In addition, the proportions of H2-Kb/OVA-specific dextramer^{+}CD8^{+} T cells and PD-1^{+}CD8^{+} T cells increased in intracranial rechallenged LL/2-OVA/Luc tumors compared with the control (**Fig. 4E and**

303 **4F**). These findings suggest that PD-1 blockade induces long-lived memory T cells and
304 antigen-specific T cells in intracranial lesions, leading to a low frequency of intracranial
305 progression in cancer immunotherapies.
306
307 **Initial rejection of subcutaneous mouse tumors after treatment with PD-1 blockade**
308 **does not suppress rechallenge of different tumors.**
309 We rechallenged different tumor cells (LL/2-OVA) subcutaneously after complete
310 rejection of subcutaneous MC-38 tumors by PD-1 blockade (**Fig. 5A**). Subcutaneously
311 different tumors were not rejected and grew comparably with the controls (**Fig. 5B**). The
312 proportions of H2-Kb/OVA-specific dextramer^{+}CD8^{+} T cells did not increase in the
313 subcutaneous rechallenged LL/2-OVA tumors (**Fig. 5C**).
314 Similarly, we rechallenged different tumor cells (LL/2-OVA/Luc) intracranially
315 after complete rejection of subcutaneous MC-38 tumors by PD-1 blockade (**Fig. 5D**). As
316 expected, different tumors were not suppressed and grew comparably with the controls
317 (**Fig. 5E**), and the proportions of H2-Kb/OVA-specific dextramer^{+}CD8^{+} T cells did not
318 increase in intracranial rechallenged LL/2-OVA/Luc tumors (**Fig. 5F**). These findings

indicate that different clones can intracranially as well as systemically relapse after the initial response to PD-1 blockade therapies.

Discussion

Although local therapies, such as stereotactic radiosurgery, surgery, and whole-brain radiation therapy, remain the mainstay of treatment for many patients with intracranial metastases, a growing number of systemic options are now available and/or are under investigation. However, several barriers in the CNS limit the access of cytotoxic drugs, mAbs, and small TKIs to intracranial metastases, leading to less efficacy for intracranial lesions and a high frequency of intracranial progression [1-5, 7-9]. On the other hand, several studies have shown that ICIs exhibit efficacy against intracranial metastases from various types of cancer, including NSCLC [16-20], which is supported by our experimental data. In addition, another study showed that the frequency of intracranial progression seemed not to be high compared with other organs during treatment with PD-1 blockade therapies [21], and our clinical data clearly demonstrated a lower frequency of

intracranial progression during treatment with PD-1 blockade therapies than platinum doublet chemotherapies. Experimentally, intracranial rechallenged tumors were suppressed after complete initial eradication by PD-1 blockade, supporting the low frequency of intracranial progression and long-term effects intracranially as well as systemically. To the best of our knowledge, our present study is the first report showing a lower frequency of intracranial progression in NSCLC during treatment with PD-1 blockade therapies, which was supported by mouse models.

Several barriers in the CNS limit effective drug delivery. The blood–brain barrier (BBB) is typical of capillaries in the normal brain: the tight junctions between endothelial cells and astrocyte–endothelial contacts, along with the multiple transport systems, regulate the passive diffusion and selective entry of compounds into the brain and, thus, water-soluble and large anticancer agents (such as mAbs) cannot cross a normal BBB [7]. Despite the limited penetration of mAbs into intracranial tumors, we revealed the intracranial efficacy of PD-1 blockade along with effector T-cell activation and cancer antigen-specific T-cell infiltration. Furthermore, we analyzed the proportion of MPECs that generate long-lived $CD8^+$ memory T cells [31], showing that MPECs were induced in

intracranial tumors as well as subcutaneous tumors by PD-1 blockade. Consistently, intracranial rechallenged tumors were suppressed, as was observed in subcutaneous tumors. Thus, even if ICIs cannot penetrate intracranial tumors, intracranial activated effector T cells and/or long-lived memory T cells induced by ICIs can lead to efficacy and long-term effects intracranially and systemically. Indeed, a previous study showed a comparable frequency of intracranial progression during treatment with PD-1 blockade therapies [21], and our clinical data clearly demonstrated less intracranial progression in NSCLC during treatment with PD-1 blockade therapies than with platinum doublet chemotherapies.

If extracranial lesions are controlled by ICI therapies as previously reported [32], it is probably difficult for them to progress to intracranial lesions with or without the BBB. However, significant intracranial tumor regression and long-term intracranial PFS were observed in several patients with initial intracranial lesions in the ICI cohort (**Supplementary Fig. S1**). By contrast, such cases were rare in the non-ICI cohort. These results support the idea that cancer immunotherapies can prevent intracranial progression and maintain long-term effects intracranially as well as systemically.

Although the frequency of intracranial progression seems to not be high, different rechallenged tumors were not suppressed in our mouse models. Thus, if intracranial recurrence occurs during the treatment with PD-1 blockade therapies, aggressive local therapies could be challenging, considering the possibility of different clones from primary tumors. Indeed, other studies have shown that local therapies in patients with intracranial progressive oligometastases with PD-1 blockade therapies can render patients disease-free [33].

NSCLC often metastasizes to the liver, bones, and brain [34, 35]. In this study, liver and bone metastases were analyzed in the same cohorts. These results suggest that the administration of ICI to patients with NSCLC may inhibit hepatic and bone progression, but not as markedly as its effect on intracranial progression. Based on previous reports, the efficacy of ICI for the treatment of liver and bone metastases may be low [36-39]. However, this was a relatively small and retrospective study, and bone progression was not accurately evaluated because we did not periodically perform bone scintigraphy or PET-CT in clinical settings; therefore, larger prospective studies are required.

This study has several limitations. Particularly, as previously mentioned, this was

a retrospective study using relatively small cohorts from a single institute, which can include some unrecognized biases. In addition, detailed clinical data after intracranial progression, such as local therapies, were not collected. Furthermore, non-ICI and ICI cohorts could not be analyzed during the same period. This is because very few patients, most of whom had autoimmune diseases, received platinum doublet chemotherapy without ICIs between 2017 and 2020. Therefore, cohorts with different enrollment times were compared. The observation period was censored at 36 months to avoid lead-time bias between the two groups. Because no major changes occurred in the treatment of *EGFR* wild-type or *ALK* wild-type advanced NSCLC other than ICIs during this period, we believe that our comparison is fair. There are also concerns regarding missing intracranial lesions. However, because MRI is widely and routinely used in Japan, all patients in both cohorts underwent MRI at diagnosis and during follow-up, minimizing the risk of missing intracranial lesions. Thus, to confirm our findings, further large cohort studies including prospective detailed ones are warranted in the future. In addition, the tumors were stereotactically transplanted into the brains of our mouse model. However, injecting tumor cells from the carotid artery or heart would be closer to clinical settings

399 [40], which is a topic for future studies.

400 In summary, we found that the frequency of intracranial progression in NSCLC
401 patients treated with PD-1 blockade therapies was significantly lower than that in those
402 treated with platinum doublet chemotherapies. In mouse models, intracranial
403 rechallenged tumors after initial eradiation by PD-1 blockade were suppressed, as was
404 observed in subcutaneous tumors. On the other hand, different rechallenged tumors were
405 not suppressed in our mouse models. Because the CNS seems to be a sanctuary site
406 against systemic therapies, intracranial lesions can be resistant to systemic therapies, and
407 NSCLC patients treated with systemic therapies, especially durable responders, tend to
408 have intracranial recurrences. However, regardless of the low penetration of drugs, our
409 results suggest that cancer immunotherapies exhibit efficacy against intracranial lesions
410 via activated effector T cells and that NSCLC patients treated with cancer
411 immunotherapies can have a lower frequency of intracranial progression via long-lived
412 memory T cells, indicating that cancer immunotherapies can maintain long-term effects
413 intracranially and systemically. If intracranial recurrence occurs during PD-1 blockade
414 therapy, it is possible that a different clone of the primary tumor is present. In this case,

aggressive local treatment may be appropriate.

Authors' contributions

NK: Methodology, Data curation, Writing- Original draft preparation. KNinomiya: Data curation, Writing- Reviewing and Editing. KKunimasa: Data curation, Writing- Reviewing and Editing. TIshino: Methodology, Data curation, Writing- Reviewing and Editing. JN: Methodology, Data curation, Writing- Reviewing and Editing. YO: Methodology, Writing- Reviewing and Editing. HM: Methodology, Writing- Reviewing and Editing. EI: Data curation, Writing- Reviewing and Editing. KO: Data curation, Writing- Reviewing and Editing. TInoue: Data curation, Writing- Reviewing and Editing. MT: Data curation, Writing- Reviewing and Editing. KS: Data curation, Writing- Reviewing and Editing. YU: Methodology, Writing- Reviewing and Editing. HD: Writing- Reviewing and Editing, Supervision. KNishio: Writing- Reviewing and Editing, Supervision. KK: Data curation, Writing- Reviewing and Editing. ID: Writing- Reviewing and Editing, Supervision. YT: Conceptualization and Project administration, Methodology, Writing- Original draft preparation. The work reported in the paper has been performed by the authors, unless clearly specified in the text.

Acknowledgements:

We thank Ms. R. Inukai, M. Iwado, Y. Nishimori, and S. Nakada for their technical assistance, and H Land, J Morgenstern, B Weinberg, and D Kotton for created plasmids. We also thank Central Research Laboratory of Okayama University Medical school for technical support.

Funding: This study was supported by

Grants-in-Aid for Scientific Research [B grant no. 20H03694 (YT) and Challenging Exploratory Research no 22K1945904 (YT)] from JSPS; the Project for Cancer Research and Therapeutic Evolution [P-CREATE, no. 21cm0106383 (YT) and no. 22ama221303h0001 (YT)]; Practical Research for Innovative Cancer Control [no. 22ck0106723h0001 (YT)]; the Core Research for Evolutional Science and Technology [CREST, no. 22gm1810002s0101 (YT)] from AMED; the Fusion Oriented Research for disruptive Science and Technology [FOREST, no. 21-211033868 (YT)] from JST; the Naito Foundation (YT); the Takeda Science Foundation (YT); the MSD Life Science Foundation (YT); the Grant for Lung Cancer Research (YT); the GSK Japan Research Grant 2021 (YT); the Astellas Foundation for Research on Metabolic Disorders (YT); the Japan Respiratory Foundation (YT); the Research Grant of the Princess Takamatsu Cancer Research Fund (YT); the Kato Memorial Bioscience Foundation (YT); the Ono Medical Research Foundation (YT); the Inamori Foundation (YT); the Ube Industries Foundation (YT); the Pharmacology Research Foundation (YT); the Suzuken Memorial Foundation (YT).

Competing interests: EI received research grants from MSD, Ono pharmaceutical, Takeda pharmaceutical, and Janssen pharmaceutical, and personal fees from Eli Lilly and Boehringer Ingelheim outside of this study. KO received research grants from Eli Lilly and Chugai Pharmaceutical outside of this study. TInoue received a personal fee from AstraZeneca outside of this study. MT received personal fees from Boehringer Ingelheim,

Chugai Pharmaceutical, AstraZeneca, Pfizer Pharmaceutical and Ono Pharmaceutical outside of this work. KNishio received research grants from Boehringer Ingelheim, West Japan Oncology Group, Thoracic Oncology Research Group, North East Japan Study Group, Clinical Research Support Center Kyushu, Nichirei Biosciences, Osakaminami hospital, Eli Lilly Japan, and Hitachi, and personal fees from Boehringer Ingelheim, AstraZeneca, Chugai Pharmaceutical, and Novartis outside of this study. ID received a research grant from Momotaro Gene outside of this study. KKiura received research grants from Taiho Pharmaceutical, Ono Pharmaceutical, Chugai Pharmaceutical, Boehringer Ingelheim, and Takeda Pharmaceutical outside of this work. YT received research grants from KOTAI Biotechnologies, Daiichi-Sankyo, Ono Pharmaceutical, Bristol-Myers Squibb, and KORTUC, and personal fees from Ono Pharmaceutical, Bristol-Myers Squibb, AstraZeneca, Chugai Pharmaceutical, MSD, and Sonire outside of this study. All other authors declare that they have no competing financial interests.

Ethics statement: The study design was approved by the appropriate ethics review board at Okayama University (2201-022). This study was conducted in accordance with the principles of the Declaration of Helsinki. Informed consent was obtained in the form of an optout on the website of our institution. Written informed consent was obtained prior to participation. Mouse experiments were approved by the Animal Committee for Animal Experimentation of Okayama University. All experiments met the U.S. Public Health Service Policy on Humane Care and Use of Laboratory Animals.

Data availability: Raw data for this study were generated at Okayama University. Derived data supporting the findings of this study are available from the corresponding author upon request.

References

1. Lin X, DeAngelis LM. Treatment of Brain Metastases. *J Clin Oncol* 2015;**33**: 3475-84.

2. Valiente M, Ahluwalia MS, Boire A, Brastianos PK, Goldberg SB, Lee EQ, Le Rhun E, Preusser M, Winkler F, Soffietti R. The Evolving Landscape of Brain Metastasis. *Trends Cancer* 2018;**4**: 176-96.

3. Mehta MP, Paleologos NA, Mikkelsen T, Robinson PD, Ammirati M, Andrews DW, Asher AL, Burri SH, Cobbs CS, Gaspar LE, Kondziolka D, Linskey ME, Loeffler JS, McDermott M, Olson JJ, Patchell RA, Ryken TC, Kalkanis SN. The role of chemotherapy in the management of newly diagnosed brain metastases: a systematic review and evidence-based clinical practice guideline. *J Neurooncol* 2010;**96**: 71-83.

4. Soffietti R, Ahluwalia M, Lin N, Rudà R. Management of brain metastases according to molecular subtypes. *Nat Rev Neurol* 2020;**16**: 557-74.

5. Soffietti R, Abacioglu U, Baumert B, Combs SE, Kinhult S, Kros JM, Marosi C, Metellus P, Radbruch A, Villa Freixa SS, Brada M, Carapella CM, Preusser M, Le Rhun E, Rudà R, Tonn JC, Weber DC, Weller M. Diagnosis and treatment of brain metastases from solid tumors: guidelines from the European Association of Neuro-Oncology (EANO). *Neuro Oncol* 2017;**19**: 162-74.

6. Markesbery WR, Brooks WH, Gupta GD, Young AB. Treatment for patients with cerebral metastases. *Arch Neurol* 1978;**35**: 754-6.

7. Kim M, Kizilbash SH, Laramy JK, Gampa G, Parrish KE, Sarkaria JN, Elmquist WF. Barriers to Effective Drug Treatment for Brain Metastases: A Multifactorial Problem in the Delivery of Precision Medicine. *Pharm Res* 2018;**35**: 177.

8. Heon S, Yeap BY, Britt GJ, Costa DB, Rabin MS, Jackman DM, Johnson BE. Development of central nervous system metastases in patients with advanced non-small cell lung cancer and somatic EGFR mutations treated with gefitinib or erlotinib. *Clin*

Cancer Res 2010;**16**: 5873-82.

9. Mamon HJ, Yeap BY, Jänne PA, Reblando J, Shrager S, Jaklitsch MT, Mentzer S, Lukanich JM, Sugarbaker DJ, Baldini EH, Berman S, Skarin A, Bueno R. High risk of brain metastases in surgically staged IIIA non-small-cell lung cancer patients treated with surgery, chemotherapy, and radiation. *J Clin Oncol* 2005;**23**: 1530-7.

10. Reck M, Rodriguez-Abreu D, Robinson AG, Hui R, Csoszi T, Fulop A, Gottfried M, Peled N, Tafreshi A, Cuffe S, O'Brien M, Rao S, Hotta K, Leiby MA, Lubiniecki GM, Shentu Y, Rangwala R, Brahmer JR, Investigators K-. Pembrolizumab versus Chemotherapy for PD-L1-Positive Non-Small-Cell Lung Cancer. *N Engl J Med* 2016;**375**: 1823-33.

11. Zou W, Wolchok JD, Chen L. PD-L1 (B7-H1) and PD-1 pathway blockade for cancer therapy: Mechanisms, response biomarkers, and combinations. *Sci Transl Med* 2016;**8**: 328rv4.

12. Jenkins RW, Barbie DA, Flaherty KT. Mechanisms of resistance to immune checkpoint inhibitors. *Br J Cancer* 2018;**118**: 9-16.

13. Ribas A, Shin DS, Zaretsky J, Frederiksen J, Cornish A, Avramis E, Seja E, Kivork C, Siebert J, Kaplan-Lefko P, Wang X, Chmielowski B, Glaspy JA, Tumeh PC, Chodon T, Pe'er D, Comin-Anduix B. PD-1 Blockade Expands Intratumoral Memory T Cells. *Cancer Immunol Res* 2016;**4**: 194-203.

14. Maio M, Grob JJ, Aamdal S, Bondarenko I, Robert C, Thomas L, Garbe C, Chiarion-Sileni V, Testori A, Chen TT, Tschaika M, Wolchok JD. Five-year survival rates for treatment-naive patients with advanced melanoma who received ipilimumab plus dacarbazine in a phase III trial. *J Clin Oncol* 2015;**33**: 1191-6.

15. Garon EB, Hellmann MD, Rizvi NA, Carcereny E, Leighl NB, Ahn MJ, Eder JP, Balmanoukian AS, Aggarwal C, Horn L, Patnaik A, Gubens M, Ramalingam SS, Felip E, Goldman JW, Scalzo C, Jensen E, Kush DA, Hui R. Five-Year Overall Survival for Patients With Advanced NonSmall-Cell Lung Cancer Treated With Pembrolizumab: Results From the Phase I KEYNOTE-001 Study. *J Clin Oncol* 2019;**37**: 2518-27.

16. Tan AC, Heimberger AB, Menzies AM, Pavlakis N, Khasraw M. Immune Checkpoint Inhibitors for Brain Metastases. *Curr Oncol Rep* 2017;**19**: 38.

17. Goldberg SB, Gettinger SN, Mahajan A, Chiang AC, Herbst RS, Sznol M, Tsiouris AJ, Cohen J, Vortmeyer A, Jilaveanu L, Yu J, Hegde U, Speaker S, Madura M, Ralabate A, Rivera A, Rowen E, Gerrish H, Yao X, Chiang V, Kluger HM.

545 Pembrolizumab for patients with melanoma or non-small-cell lung cancer and untreated
546 brain metastases: early analysis of a non-randomised, open-label, phase 2 trial. *The*
547 *Lancet Oncology* 2016;**17**: 976-83.
548 18. Goldberg SB, Schalper KA, Gettinger SN, Mahajan A, Herbst RS, Chiang
549 AC, Lilenbaum R, Wilson FH, Omay SB, Yu JB, Jilaveanu L, Tran T, Pavlik K, Rowen
550 E, Gerrish H, Komlo A, Gupta R, Wyatt H, Ribeiro M, Kluger Y, Zhou G, Wei W, Chiang
551 VL, Kluger HM. Pembrolizumab for management of patients with NSCLC and brain
552 metastases: long-term results and biomarker analysis from a non-randomised, open-label,
553 phase 2 trial. *The Lancet Oncology* 2020;**21**: 655-63.
554 19. Paz-Ares LG, Ciuleanu T-E, Cobo M, Bennouna J, Schenker M, Cheng Y,
555 Juan-Vidal O, Mizutani H, Lingua A, Reyes-Cosmelli F, Reinmuth N, Menezes J, Jassem
556 J, Protsenko S, Richardet E, Felip E, Feeney K, Zurawski B, Alexandru A, de la Mora
557 Jimenez E, Dakhil S, Lu S, Reck M, John T, Hu N, Zhang X, Sylvester J, Eccles LJ,
558 Grootendorst DJ, Balli D, Neely J, Carbone DP. First-Line Nivolumab Plus Ipilimumab
559 With Chemotherapy Versus Chemotherapy Alone for Metastatic NSCLC in CheckMate
560 9LA: 3-Year Clinical Update and Outcomes in Patients With Brain Metastases or Select
561 Somatic Mutations. *Journal of Thoracic Oncology* 2023;**18**: 204-22.
562 20. Reck M, Ciuleanu TE, Lee JS, Schenker M, Zurawski B, Kim SW, Mahave
563 M, Alexandru A, Peters S, Pluzanski A, Caro RB, Linardou H, Burgers JA, Nishio M,
564 Martinez-Marti A, Azuma K, Axelrod R, Paz-Ares LG, Ramalingam SS, Borghaei H,
565 O'Byrne KJ, Li L, Bushong J, Gupta RG, Grootendorst DJ, Eccles LJ, Brahmer JR.
566 Systemic and Intracranial Outcomes With First-Line Nivolumab Plus Ipilimumab in
567 Patients With Metastatic NSCLC and Baseline Brain Metastases From CheckMate 227
568 Part 1. *J Thorac Oncol* 2023.
569 21. Hosoya K, Fujimoto D, Morimoto T, Kumagai T, Tamiya A, Taniguchi Y,
570 Yokoyama T, Ishida T, Matsumoto H, Hirano K, Kominami R, Tomii K, Suzuki H,
571 Hirashima T, Tanaka S, Uchida J, Morita M, Kanazu M, Mori M, Nagata K, Fukuda I,
572 Tamiya M. Clinical factors associated with shorter durable response, and patterns of
573 acquired resistance to first-line pembrolizumab monotherapy in PD-L1-positive non-
574 small-cell lung cancer patients: a retrospective multicenter study. *BMC Cancer* 2021;**21**:
575 346.
576 22. Hotta K, Takigawa N, Hisamoto-Sato A, Ichihara E, Kudo K, Uchida K,
577 Yanase-Nakamura K, Tanaka H, Kato Y, Tabata M, Tanimoto M, Kiura K. Reappraisal of

578 short-term low-volume hydration in cisplatin-based chemotherapy: results of a
579 prospective feasibility study in advanced lung cancer in the Okayama Lung Cancer Study
580 Group Trial 1002. *Jpn J Clin Oncol* 2013;**43**: 1115-23.
581 23. Ninomiya K, Hotta K, Hisamoto-Sato A, Ichihara E, Gotoda H, Morichika
582 D, Tamura T, Kayatani H, Minami D, Kubo T, Tabata M, Tanimoto M, Kiura K. Short-
583 term low-volume hydration in cisplatin-based chemotherapy for patients with lung
584 cancer: the second prospective feasibility study in the Okayama Lung Cancer Study
585 Group Trial 1201. *Int J Clin Oncol* 2016;**21**: 81-7.
586 24. JP. M, H. L. Advanced mammalian gene transfer- high titre retroviral
587 vectors with multiple drug selection markers and a complementary helper-free packaging
588 cell line. *Nucleic Acids Res* 1990;**18**: 3587–96.
589 25. Wilson AA, Murphy GJ, Hamakawa H, Kwok LW, Srinivasan S, Hovav AH,
590 Mulligan RC, Amar S, Suki B, Kotton DN. Amelioration of emphysema in mice through
591 lentiviral transduction of long-lived pulmonary alveolar macrophages. *J Clin Invest*
592 2010;**120**: 379-89.
593 26. Nagasaki J, Inozume T, Sax N, Ariyasu R, Ishikawa M, Yamashita K,
594 Kawazu M, Ueno T, Irie T, Tanji E, Morinaga T, Honobe A, Ohnuma T, Yoshino M, Iwata
595 T, Kawase K, Sasaki K, Hanazawa T, Kochin V, Kawamura T, Matsue H, Hino M, Mano
596 H, Suzuki Y, Nishikawa H, Togashi Y. PD-1 blockade therapy promotes infiltration of
597 tumor-attacking exhausted T cell clonotypes. *Cell Rep* 2022;**38**: 110331.
598 27. Kawashima S, Inozume T, Kawazu M, Ueno T, Nagasaki J, Tanji E, Honobe
599 A, Ohnuma T, Kawamura T, Umeda Y, Nakamura Y, Kawasaki T, Kiniwa Y, Yamasaki O,
600 Fukushima S, Ikehara Y, Mano H, Suzuki Y, Nishikawa H, Matsue H, Togashi Y.
601 TIGIT/CD155 axis mediates resistance to immunotherapy in patients with melanoma
602 with the inflamed tumor microenvironment. *J Immunother Cancer* 2021;**9**.
603 28. Ge M, Zhuang Y, Zhou X, Huang R, Liang X, Zhan Q. High probability and
604 frequency of EGFR mutations in non-small cell lung cancer with brain metastases. *J*
605 *Neurooncol* 2017;**135**: 413-8.
606 29. Sugiyama E, Togashi Y, Takeuchi Y, Shinya S, Tada Y, Kataoka K, Tane K,
607 Sato E, Ishii G, Goto K, Shintani Y, Okumura M, Tsuboi M, Nishikawa H. Blockade of
608 EGFR improves responsiveness to PD-1 blockade in. *Sci Immunol* 2020;**5**.
609 30. Gainor JF, Shaw AT, Sequist LV, Fu X, Azzoli CG, Piotrowska Z, Huynh
610 TG, Zhao L, Fulton L, Schultz KR, Howe E, Farago AF, Sullivan RJ, Stone JR,

611 Digumarthy S, Moran T, Hata AN, Yagi Y, Yeap BY, Engelman JA, Mino-Kenudson M.
612 EGFR Mutations and ALK Rearrangements Are Associated with Low Response Rates to
613 PD-1 Pathway Blockade in Non-Small Cell Lung Cancer: A Retrospective Analysis. *Clin*
614 *Cancer Res* 2016;**22**: 4585-93.
615 31. Joshi NS, Cui W, Chandele A, Lee HK, Urso DR, Hagman J, Gapin L,
616 Kaech SM. Inflammation directs memory precursor and short-lived effector CD8(+) T
617 cell fates via the graded expression of T-bet transcription factor. *Immunity* 2007;**27**: 281-
618 95.
619 32. Gandhi L, Rodriguez-Abreu D, Gadgeel S, Esteban E, Felip E, De Angelis
620 F, Domine M, Clingan P, Hochmair MJ, Powell SF, Cheng SY, Bischoff HG, Peled N,
621 Grossi F, Jennens RR, Reck M, Hui R, Garon EB, Boyer M, Rubio-Viqueira B, Novello
622 S, Kurata T, Gray JE, Vida J, Wei Z, Yang J, Raftopoulos H, Pietanza MC, Garassino MC,
623 Investigators K-. Pembrolizumab plus Chemotherapy in Metastatic Non-Small-Cell Lung
624 Cancer. *N Engl J Med* 2018;**378**: 2078-92.
625 33. Kagawa Y, Furuta H, Uemura T, Watanabe N, Shimizu J, Horio Y, Kuroda
626 H, Inaba Y, Kodaira T, Masago K, Fujita S, Niimi A, Hida T. Efficacy of local therapy for
627 oligoprogressive disease after programmed cell death 1 blockade in advanced non-small
628 cell lung cancer. *Cancer Sci* 2020;**111**: 4442-52.
629 34. Riihimaki M, Hemminki A, Fallah M, Thomsen H, Sundquist K, Sundquist
630 J, Hemminki K. Metastatic sites and survival in lung cancer. *Lung Cancer* 2014;**86**: 78-
631 84.
632 35. Tamura T, Kurishima K, Nakazawa K, Kagohashi K, Ishikawa H, Satoh H,
633 Hizawa N. Specific organ metastases and survival in metastatic non-small-cell lung
634 cancer. *Mol Clin Oncol* 2015;**3**: 217-21.
635 36. Topalian SL, Hodi FS, Brahmer JR, Gettinger SN, Smith DC, McDermott
636 DF, Powderly JD, Sosman JA, Atkins MB, Leming PD, Spigel DR, Antonia SJ, Drilon A,
637 Wolchok JD, Carvajal RD, McHenry MB, Hosein F, Harbison CT, Grosso JF, Sznol M.
638 Five-Year Survival and Correlates Among Patients With Advanced Melanoma, Renal Cell
639 Carcinoma, or Non-Small Cell Lung Cancer Treated With Nivolumab. *JAMA Oncol*
640 2019;**5**: 1411-20.
641 37. Rodriguez-Abreu D, Powell SF, Hochmair MJ, Gadgeel S, Esteban E, Felip
642 E, Speranza G, De Angelis F, Domine M, Cheng SY, Bischoff HG, Peled N, Reck M, Hui
643 R, Garon EB, Boyer M, Kurata T, Yang J, Pietanza MC, Souza F, Garassino MC.

Pemetrexed plus platinum with or without pembrolizumab in patients with previously untreated metastatic nonsquamous NSCLC: protocol-specified final analysis from KEYNOTE-189. *Ann Oncol* 2021;**32**: 881-95.

38. Landi L, D'Inca F, Gelibter A, Chiari R, Grossi F, Delmonte A, Passaro A, Signorelli D, Gelsomino F, Galetta D, Giannarelli D, Soto Parra H, Minuti G, Tiseo M, Migliorino MR, Cognetti F, Toschi L, Bidoli P, Piantedosi F, Calabro L, Cappuzzo F. Bone metastases and immunotherapy in patients with advanced non-small-cell lung cancer. *J Immunother Cancer* 2019;**7**: 316.

39. Tumeh PC, Hellmann MD, Hamid O, Tsai KK, Loo KL, Gubens MA, Rosenblum M, Harview CL, Taube JM, Handley N, Khurana N, Nosrati A, Krummel MF, Tucker A, Sosa EV, Sanchez PJ, Banayan N, Osorio JC, Nguyen-Kim DL, Chang J, Shintaku IP, Boasberg PD, Taylor EJ, Munster PN, Algazi AP, Chmielowski B, Dummer R, Grogan TR, Elashoff D, Hwang J, Goldinger SM, Garon EB, Pierce RH, Daud A. Liver Metastasis and Treatment Outcome with Anti-PD-1 Monoclonal Antibody in Patients with Melanoma and NSCLC. *Cancer Immunol Res* 2017;**5**: 417-24.

40. Liu Z, Wang Y, Kabraji S, Xie S, Pan P, Liu Z, Ni J, Zhao JJ. Improving orthotopic mouse models of patient-derived breast cancer brain metastases by a modified intracarotid injection method. *Sci Rep* 2019;**9**: 622.

664 **Figure legends**

665 **Figure 1. Intracranial PFS curves.**

666 Patients who received standard platinum doublet chemotherapies (N = 32) or PD-1
667 blockade therapies without anti-CTLA-4 mAb (N = 54) as first-line therapies were
668 enrolled in this study as the non-ICI and ICI cohorts, respectively. Contrast-enhanced
669 MRI of the brain was performed before and at least every six months after
670 chemotherapy. For intracranial progression, RECIST ver. 1.1 was applied. For clinical
671 intracranial progression, an event was defined as the date of imaging. Intracranial PFS
672 was defined as the time from the initiation of first-line standard chemotherapy to the
673 first observation of intracranial disease progression or death from any cause.
674 Intracranial PFS curves for all patients (**A**), patients with non-SQ histologies (**B**), and
675 patients without initial intracranial lesions (**C**) are shown.
676
677 Intracranial PFS was analyzed using the Kaplan–Meier method and compared among
678 groups using the log-rank test. *, $P < 0.05$.
679
680 **Figure 2. *In vivo* efficacy of PD-1 blockade against LL2-OVA tumors.**
681 **(A)** *In vivo* efficacy of PD-1 blockade against subcutaneous LL2-OVA tumors. LL2-
682 OVA cells (5×10^6) were inoculated subcutaneously on Day 0 (n = 6 per group), and
683 tumor volume was monitored every three days. The means of the long and short
684 diameters were used to generate tumor growth curves. Anti-PD-1 mAb was
685 administered on Days 4, 7, and 10.

(B) *In vivo* efficacy of PD-1 blockade against intracranial LL2-OVA/Luc tumors. LL2-OVA/Luc cells (2×10^5) were stereotactically injected into the striatum on Day 0 (n = 5 per group). Anti-PD-1 mAb was administered on Days 4, 7, and 10. IVIS was used for imaging intracranial tumors on Day 14. Representative imaging and the summary are shown.

(C) and **(D)** The proportions of $CD44^+CD62L^-CD8^+$ T cells (C) and $PD\text{-}1^+CD8^+$ T cells (D) in intracranial LL/2-OVA tumors. Mouse experiments were performed as described in (B), and tumors were harvested on Day 14 for evaluation by flow cytometry (n = 5 per group). Representative flow cytometry staining (left) and summaries (right) are shown.

All *in vivo* experiments were performed in duplicate, with similar results. Two-way ANOVA was used in (A) and t tests were used in (B)-(D) for statistical analyses. The means and SEMs are shown. *, $P < 0.05$.

Figure 3. Subcutaneous rechallenges with the same LL/2-OVA tumor cells in mice treated with PD-1 blockade.

(A) Experimental schema. Mice that had completely eradicated the initial subcutaneous tumors after anti–PD-1 mAb were subcutaneously rechallenged with same tumor cells on Day 32.

(B) Volume of each rechallenged LL2-OVA tumor. The means of the long and short diameters were used to generate tumor growth curves, and the volume of each tumor is

shown (n = 10 per group). CR, complete rejection.

(C) and **(D)** The proportions of $CD127^{+}KLRG1^{-}$MEPCs (C) and H2-Kb/OVA-specific $dextramer^{+}CD8^{+}$ T cells (D) in subcutaneous LL/2-OVA tumors. Mouse experiments were performed as described in **Figure 2A**, and tumors were harvested on Day 14 for evaluation by flow cytometry (n = 5 per group). Representative flow cytometry staining (left) and summaries (right) are shown.

All *in vivo* experiments were performed in duplicate, with similar results. T tests were used in (C) and (D) for statistical analyses. The means and SEMs are shown. *, $P < 0.05$; ***, $P < 0.001$.

Figure 4. Intracranial rechallenges with the same LL/2-OVA tumor cells in mice treated with PD-1 blockade.

(A) Experimental schema. Mice that had completely eradicated the initial subcutaneous tumors after anti–PD-1 mAb were intracranially rechallenged with same tumor cells on Day 32.

(B) Intracranial rechallenge of LL2-OVA/Luc tumor growth. IVIS was used for imaging of intracranial tumors on Day 46 (n = 5 per group). Representative imaging and the summary are shown.

(C) and **(D)** The proportions of $CD127^{+}KLRG1^{-}$MEPCs (C) and H2-Kb/OVA-specific $dextramer^{+}CD8^{+}$ T cells (D) in intracranial LL/2-OVA/Luc tumors. Mouse experiments were performed as described in **Figure 2B**, and tumors were harvested on Day 14 for

evaluation by flow cytometry (n = 5 per group). Representative flow cytometry staining (left) and summaries (right) are shown.

(E) and (F) The proportion of H2-Kb/OVA-specific dextramer^{+}CD8^{+} T cells (E) and PD-1^{+}CD8^{+} T cells (F) in intracranial rechallenged LL/2-OVA/Luc tumors. Rechallenged LL2-OVA/Luc tumors were harvested on Day 46 for evaluation by flow cytometry (n = 5 per group). Representative flow cytometry staining (left) and summaries (right) are shown.

All *in vivo* experiments were performed in duplicate, with similar results. T tests were used in (B)-(F) for statistical analyses. The means and SEMs are shown. *, $P < 0.05$; **, $P < 0.01$; ***, $P < 0.001$.

Figure 5. Subcutaneous or intracranial different tumor rechallenge in mice treated with PD-1 blockade.

(A) Experimental schema. Mice that had completely eradicated the initial subcutaneous tumors (MC-38) after anti–PD-1 mAb were subcutaneously rechallenged with different tumor cells (LL2-OVA) on Day 32.

(B) Volume of each subcutaneous rechallenged LL2-OVA tumor. The means of the long and short diameters were used to generate tumor growth curves, and the volume of each tumor is shown (n = 10 per group). CR, complete rejection.

(C) The proportion of H2-Kb/OVA-specific dextramer^{+}CD8^{+} T cells in subcutaneous rechallenged LL/2-OVA tumors. Subcutaneous rechallenged LL/2-OVA tumors were

harvested on Day 46 for evaluation by flow cytometry (n = 5 per group). Representative flow cytometry staining (left) and summaries (right) are shown.

(D) Experimental schema. Mice that had completely eradicated the initial subcutaneous tumors (MC-38) after anti–PD-1 mAb were intracranially rechallenged with different tumor cells (LL2-OVA/Luc) on Day 32.

(E) Intracranial rechallenge of LL2-OVA/Luc tumor growth. IVIS was used for imaging of intracranial tumors on Day 46 (n = 5 per group). Representative imaging and the summary are shown.

(F) The proportion of H2-Kb/OVA-specific dextramer^{+}CD8^{+} T cells in intracranial rechallenged LL/2-OVA/Luc tumors. Intracranial rechallenged LL/2-OVA/Luc tumors were harvested on Day 46 for evaluation by flow cytometry (n = 5 per group). Representative flow cytometry staining (left) and summaries (right) are shown.

All *in vivo* experiments were performed in duplicate, with similar results. T tests were used in (C), (E), and (F) for statistical analyses. The means and SEMs are shown. n.s., not significant.

Low frequency of intracranial progression in advanced NSCLC patients treated with cancer immunotherapies

Short Title: Cancer immunotherapy and intracranial progression

Authors: Naoya Kemmotsu, Kiichiro Ninomiya, Kei Kunimasa, Takamasa Ishino, Joji Nagasaki, Yoshihiro Otani, Hiroyuki Michiue, Eiki Ichihara, Kadoaki Ohashi, Takako Inoue, Motohiro Tamiya, Kazuko Sakai, Youki Ueda, Hiromichi Dansako, Kazuto Nishio, Katsuyuki Kiura, Isao Date, and Yosuke Togashi

Table of contents

Supplementary Figure S1. Gadolinium-enhanced brain magnetic resonance image (MRI)

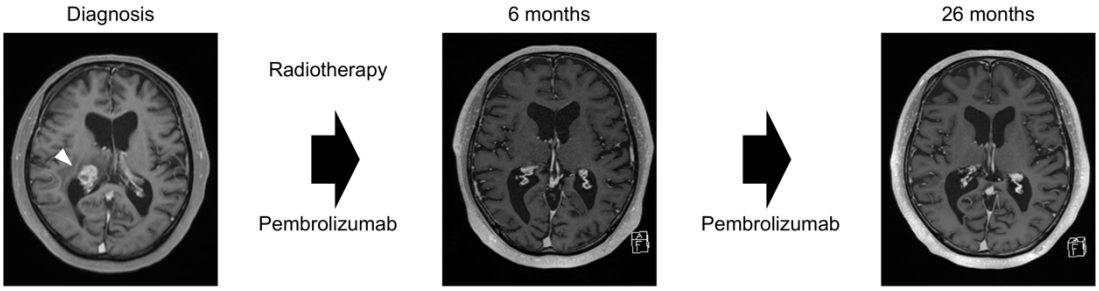

Sixty-eight-year-old male patient with non-squamous NSCLC underwent pembrolizumab as first-line chemotherapy. This patient received radiotherapy two weeks before the treatment.

Supplementary Figure S2. Additional analyses for PFS and OS

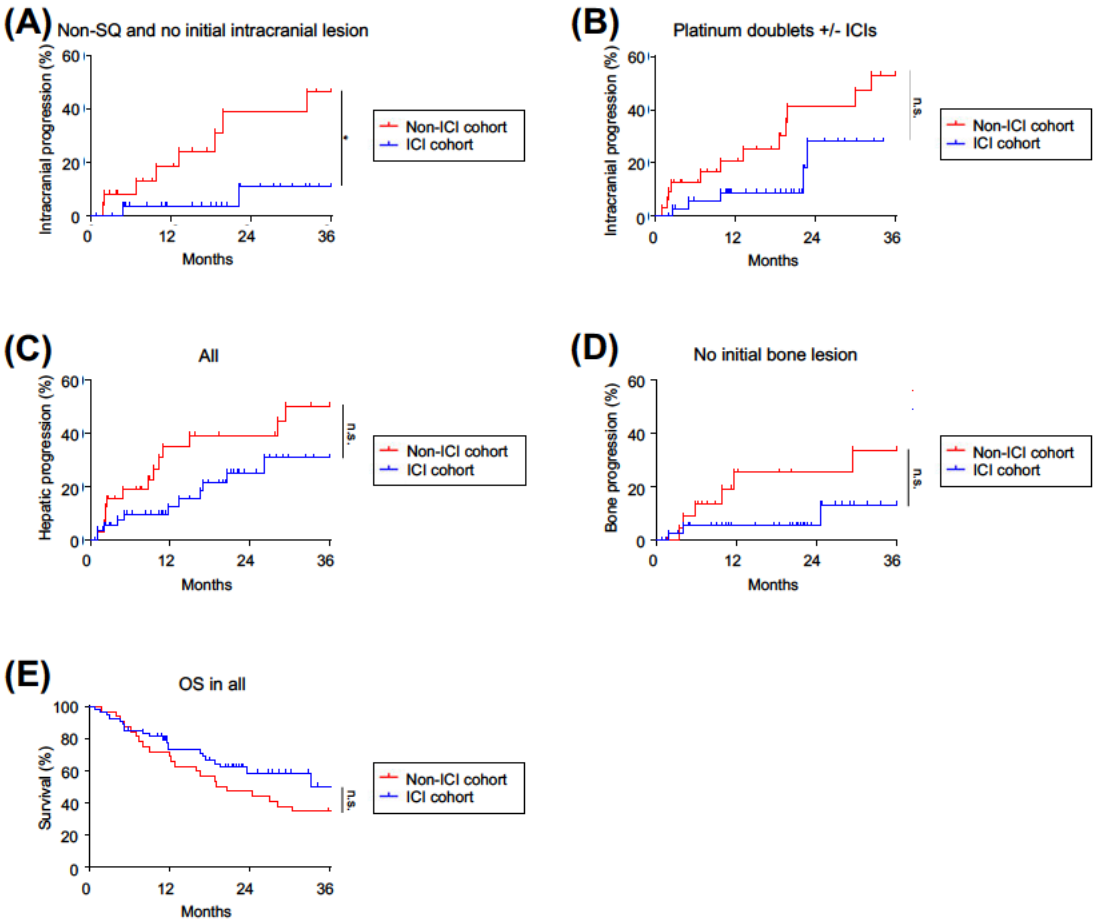

Patients who received standard platinum-doublet chemotherapies (N = 32) or PD-1 blockade therapies without anti-CTLA-4 mAb (N = 54) as first-line therapies were enrolled in this study as the non-ICI and ICI cohorts, respectively. OS, intracranial, hepatic, and bone progression-free survival (PFS) were defined as the time from the initiation of first-line standard chemotherapy to death from any cause, the time from the initiation of first-line standard chemotherapy to the first observation of intracranial disease progression or death from any cause, the time from the initiation of first-line standard chemotherapy to the first observation of hepatic disease progression or death from any cause, and the time from the initiation of first-line standard chemotherapy to the first observation of bone disease progression or death from any cause, respectively. Intracranial PFS curves for patients with non-SQ without initial intracranial lesions and patients received platinum doublet +/- ICI therapies are shown in **(A)** and **(B)**, respectively. Hepatic PFS curves for all patients and bone PFS curves for patients without initial bone lesions are shown in **(C)** and **(D)**, respectively. OS of all patients is shown in **(E)**.

PFS and OS was analyzed using the Kaplan–Meier method and compared among groups using the log-rank test. *, $P < 0.05$; n.s., not significant.

Supplementary Figure S3. *In vivo* efficacy of PD-1 blockade against MC-38 tumors

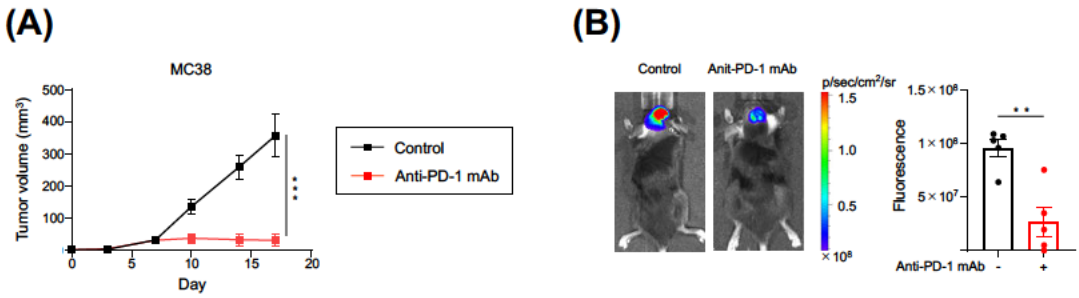

(A) *In vivo* efficacy of PD-1 blockade against subcutaneous MC-38 tumors. Mouse experiments were performed as described in **Figure 2A**.

(B) *In vivo* efficacy of PD-1 blockade against intracranial MC-38 tumors. Mouse experiments were performed as described in **Figure 2B**, and IVIS was used for imaging intracranial tumors on Day 14. Representative imaging and the summary are shown.

All *in vivo* experiments were performed in duplicate, with similar results. Two-way ANOVA was used in (A), and a t test was used in (B) for statistical analyses. The means and SEMs are shown. **, $P < 0.01$; ***, $P < 0.001$.

Supplementary Figure S4. TIL analyses in subcutaneous LL/2-OVA tumors

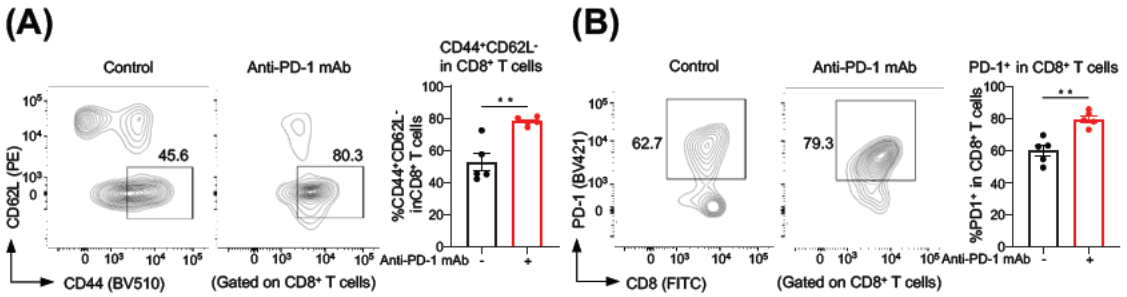

The proportions of $CD44^+CD62L^-CD8^+$ T cells (A) and $PD\text{-}1^+CD8^+$ T cells (B) in subcutaneous LL/2-OVA tumors. Mouse experiments were performed as described in **Figure 2A**, and tumors were harvested on Day 14 for evaluation by flow cytometry (n = 5 per group). Representative flow cytometry staining (left) and summaries (right) are shown.

All *in vivo* experiments were performed in duplicate, with similar results. T tests were used for statistical analyses. The means and SEMs are shown. **, $P < 0.01$.

Supplementary Figure S5. Rechallenges with the same MC-38 tumor cells in mice treated with PD-1 blockade

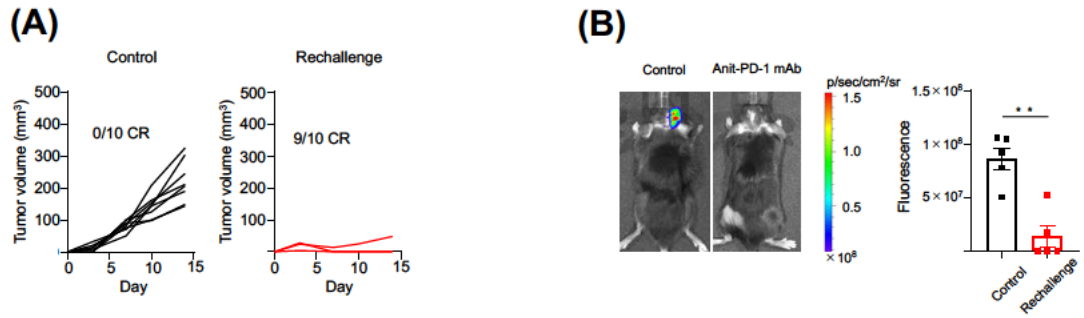

(A) Volume of each rechallenged MC-38 tumor. Mice that had completely eradicated the initial subcutaneous tumors after anti–PD-1 mAb were subcutaneously rechallenged with the same tumor cells on Day 32 (n = 10 per group). The means of the long and short diameters were used to generate tumor growth curves, and the volume of each tumor is shown. CR, complete rejection.

(B) Intracranial rechallenge of MC-38/Luc tumor growth. Mice that had completely eradicated the initial subcutaneous tumors after anti–PD-1 mAb were intracranially rechallenged with the same tumor cells on Day 32 (n = 5 per group). IVIS was used for imaging intracranial tumors on Day 46. Representative imaging and the summary are shown.

All *in vivo* experiments were performed in duplicate, with similar results. A t test was used in (B) for statistical analysis. The means and SEMs are shown. **, $P < 0.01$.

Supplementary Table S1. Patient characteristics

Features	Non-ICI cohort (n = 32)	ICI cohort (n = 54)	*P*
Age, years [median] (range)	62 (48–73)	68.5 (46–94)	0.011
Sex (male/female)	26/6	44/10	0.978
Performance status (0/1 or 2)	32/0	50/4	0.114
Histology (SQ/non-SQ)	1/31	17/37	0.001
Initial intracranial lesions (yes/no)	6/26	8/46	0.632
Initial hepatic lesions (yes/no)	3/29	4/50	0.747
Initial bone lesions (yes/no)	9/23	14/40	0.823
First line therapy (Platinum doublet/PD-1 blockade alone/PD-1 blockade + platinum)	32/0/0	0/18/36	-

ICI, immune checkpoint inhibitor; SQ, squamous cell carcinoma; CNS, central nervous system.

867 **Supplementary Table S2. Summary of antibodies used in flow cytometry analyses**

Molecule	Tag	Clone	Company
CD3	Alexa Fluor 700	500A2	BD bioscience
CD4	PerCP-Cy5.5	RM4-5	BD bioscience
CD8a	FITC	53-6.7	BD bioscience
CD44	BV510	IM7	BD bioscience
CD62L	PE	MEL-14	BD bioscience
CD127	PE-CF594	SB/199	BD bioscience
KLRG1	PE-Cy7	2F1	eBioscience
CD279	BV421	J43	BD bioscience
H-2K^{b}-SIINFEKL	APC	-	Immudex
Fixable Viability Dye	APC-Cy7	-	eBioscience

868

869